PHYSICAL REVIEW D **79,** 053008 (2009)

Cross sections and energy loss for lepton pair production in muon transport

Alexander Bulmahn and Mary Hall Reno

Department of Physics and Astronomy, University of Iowa, Iowa City, Iowa 52242, USA

(Received 30 December 2008; published 20 March 2009)

We reevaluate electron-positron pair production from electromagnetic interactions of muons in transit through materials. Our approach, through the use of structure functions for inelastic and elastic scattering and including hadronic recoil, make the formalism useful for tau pair production at high energies. Our results for electron-positron pairs agree well with prior evaluations. Tau pair production, however, has significant contributions from inelastic scattering in addition to the usual coherent scattering with the nucleus and scattering with atomic electrons.

DOI: 10.1103/PhysRevD.79.053008 PACS numbers: 13.60.−r, 13.85.Tp

I. INTRODUCTION

Atmospheric muons, the muons produced by cosmic ray interactions in the Earth, are detected by many underground detectors. Downward-going muons are a large background to neutrino induced events [1–4]. For a range of energies, measurements of muon fluxes test our understanding of the underlying interactions that produce the muons and offer the opportunity to test models of the cross section for cosmic ray interactions with air nuclei.

Measurements of the energy dependence of the atmospheric lepton fluxes rely on knowledge of the muon energy loss as a function of distance. Underground and underwater detectors can effectively probe atmospheric muon energies by looking at the muon flux as a function of zenith angle θ. Vertical muons travel a depth D, while muons incident at angle θ travel a distance $\sim D/\cos\theta$. The electromagnetic energy loss is essential to the unfolding process between detected and surface muon fluxes [5,6].

In this paper, we reevaluate the cross section for muon-atom scattering to produce lepton pairs, and the energy loss of muons from the production of electron-positron pairs. The largest contribution to the muon energy loss parameter β in the energy loss formula

$$\left\langle \frac{dE}{dX} \right\rangle = -(\alpha + \beta E) \tag{1}$$

comes from pair production [7–10]. The ''pair-meter'' method of muon energy determination also relies on the e^+e^- pair production cross section [11–13].

Evaluations of muon cross sections and energy loss from pair production in collisions of a muon and a static nucleus have a long history [14–27]. In this paper, we present the cross section in terms of form factors and structure functions [19] that are not restricted to low lepton masses or low momentum transfers to the target. We include target recoil in the kinematics [20], and the inelastic contribution [22,25] to the cross section and energy loss parameter $\beta_{\rm pair}$ using structure functions parametrized from HERA data [28,29]. Our results are compared with the commonly used parametrization of Kokoulin and Petrukhin [18]. We do not address the production of muon pairs because of the extra contributions from having identical particles in the final state [23–27].

We begin by reviewing the calculation in a formalism applicable to elastic and inelastic scattering including the hadronic recoil. We show the standard generalization to atoms. Our results for the cross section and energy loss parameter β for protons, hydrogen, and higher Z atoms are shown in Sec. III. In Sec. IV we show an application to high energy e^+e^- and $\tau^+\tau^-$ pairs. Many of the calculational details are relegated to the appendix.

II. NOTATION AND FORMALISM

Our organization of the matrix element squared follows the notation of Kel'ner in Ref. [16]; however, here we include target recoil. Akhundov, Bardin, and Shumeiko evaluated lepton pair production in μp scattering with proton recoil in Ref. [20]. We follow their notation for the kinematics.

For definiteness, we begin with e^+e^- pair production. The incident muon with four-momentum k interacts with a nucleus of four-momentum p. The outgoing muon (k_1), electron (k_2), and positron (k_3) are accompanied by a hadronic final state with $p_H = \sum_{x=\rm hadrons} p_x$. The Appendix includes the definition of relevant Lorentz scalars. Note that $p^2 = M_t^2$ is the target mass squared, $k^2 = k_1^2 = m_\mu^2$ and $k_2^2 = k_3^2 = m_e^2$. When the target is a proton or a neutron, we set $M_t = M$.

There are a number of diagrams that contribute to e^+e^- pair production. For μp scattering, there are diagrams where a virtual photon radiated from the muon or proton splits directly into an e^+e^- pair. The dominant contributions to the pair production cross section come from the two diagrams shown in Fig. 1 [17,25,26]. As a simplification, we include only the diagrams in Fig. 1 in our evaluation.

The strategy to evaluate the differential cross section is outlined in Kel'ner [16], and extended here to include the inelastic case including recoil of the final state hadrons. The hadronic matrix element squared $H^{\mu\nu}$ is related to a

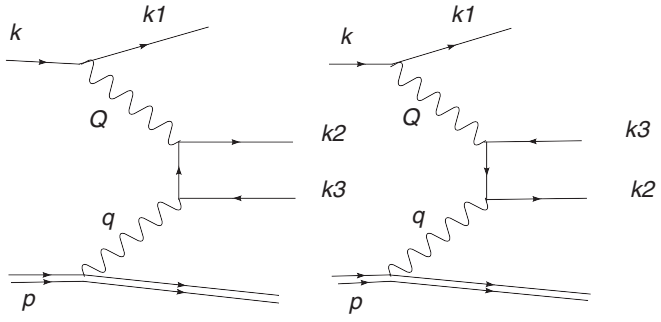

FIG. 1. The dominant contribution in μp production of e^+e^- pair production comes from virtual photon graphs shown here. The figure was produced using JAXODRAW [42].

decomposition into structure functions F_1 and F_2 which depend on $q^2 = (p - p_x)^2 \equiv -t$ and $x_{Bj} = q^2/2p \cdot q$ [30]:

$$\begin{aligned} e^2 H^{\mu\nu} &= \frac{1}{2} \sum_{\text{spins},X} \langle X|J^\mu|p\rangle\langle X|J^\nu|p\rangle^* \\ W^{\mu\nu} &\equiv \frac{1}{4\pi} \int H^{\mu\nu}(2\pi)^4 \delta^4\Big(p - q - \sum p_x\Big) \\ &\quad \cdot \prod_x \frac{d^3 p_x}{2E_x(2\pi)^3} \\ &= -g^{\mu\nu} W_1 + p^\mu p^\nu \frac{W_2}{M_t^2} \\ &= -g^{\mu\nu} F_1 + \frac{p^\mu p^\nu}{M_t^2} \frac{2M_t^2 x_{Bj}}{t} F_2. \end{aligned}$$

Our choice for the sign of the four-momentum q is opposite that of the usual choice for inelastic scattering with protons.

The formalism in terms of $W^{\mu\nu}$ is relevant to both inelastic and elastic scattering. For inelastic scattering, F_1 and F_2 are dependent on x_{Bj} and t independently. For elastic scattering, $x_{Bj} = 1$ and F_1 and F_2 are proportional to the delta function $\delta(t + 2p \cdot q) = \delta(M_X^2 - M_t^2)$, where we have made the assignment $(\sum p_x)^2 = M_X^2$.

The spin averaged matrix element squared for the muon part of the diagram is

$$A_{\alpha\beta} = \tfrac{1}{2}\text{Tr}(\not{k}_1 + m_\mu)\gamma_\alpha(\not{k} + m_\mu)\gamma_\beta. \tag{2}$$

The change in muon momentum is defined to be $Q \equiv k - k_1$ with $Q^2 = -Y$.

The $\gamma^*(Q) + \gamma^*(q) \to e(k_2) + \bar{e}(k_3)$ matrix element comes from the two diagrams shown in Fig. 1. The result is represented by $e^4 B^{\alpha\beta}_{\mu\nu}$, so that the differential cross section can be written as

$$\begin{aligned} d\sigma = \frac{1}{2\sqrt{\lambda_s}} A_{\alpha\beta} B^{\alpha\beta}_{\mu\nu} \frac{e^8}{t^2 Y^2} \delta^4\Big(k + q - \sum_{i=1}^{3} k_i\Big) \prod_i \frac{d^3 k_i}{2E_i(2\pi)^3} \\ \times 4\pi W^{\mu\nu} d^4 q, \end{aligned} \tag{3}$$

where $\lambda_s = (2p \cdot k)^2 - 4m_\mu^2 M_t^2$.

The details of the phase space integrals are in the Appendix; however, because of its length, we have not included an explicit expression for $B^{\alpha\beta}_{\mu\nu}$. We have evaluated $B^{\alpha\beta}_{\mu\nu}$ using the symbolic manipulation program FORM [31]. We follow Kel'ner's calculational simplifications [16] by projecting out different terms in the matrix element squared integrated over most of the phase space. Ultimately, we evaluate numerically $d\sigma/dy$, σ, and

$$\beta_{\text{pair}} \equiv \frac{N_A}{A} \int y \frac{d\sigma}{dy} dy, \tag{4}$$

where $y \equiv p \cdot Q/p \cdot k$ is the usual inelasticity parameter and $d\sigma/dy$ is the differential cross section for e^+e^- pair production. In the target rest frame, $p = (M_t, 0, 0, 0)$, $y = (E - E_1)/E$, the difference in incoming and outgoing muon energies, normalized by the incoming muon energy. In Eq. (4), N_A is Avogadro's number and A is the atomic mass.

The structure functions F_1 and F_2 carry information about the nucleus as well as about the electron cloud which screens the nucleus. We discuss the elastic and inelastic cases separately in the next sections. It is convenient to further divide the contributions to the cross section according to the dependence on the nuclear charge Z.

A. Coherent scattering with the screened nucleus

Coherent scattering with the nucleus amounts to elastic scattering with the charge Z nucleus of mass $M_t = M_A = AM$, leading to a factor of Z^2. As we show below, for elastic scattering, a delta function enforcing $M_X^2 = M_A^2$ ($t = -2p \cdot q$) appears in the structure functions.

For coherent scattering with an atom of mass M_A, atomic mass A, and charge Z, the structure functions in the standard approach are written in terms of $\tau \equiv t/(4M_A^2)$:

$$F_1^{\text{coh}} = \frac{t}{2} G_M^2 \delta(M_X^2 - M_A^2), \tag{5}$$

$$F_2^{\text{coh}} = \frac{t}{1+\tau}((G_E - F_e)^2 + \tau G_M^2)\delta(M_X^2 - M_A^2). \tag{6}$$

The electric form factor $G_E(t)$ accounts for the electric charge distribution in the nucleus, with $G_E(0) = Z$, whereas $F_e(t)$ accounts for the Z electrons in the atom which screen the nucleus at large distances.

We begin with the nucleon form factors, following with nuclear form factors. A recent review of the elastic form factors appears in Ref. [32]. Traditionally, the electric and magnetic form factors (G_E and G_M) are written in dipole form. For the proton

$$G(t) = \frac{1}{(1 + t/0.71\ \mathrm{GeV}^2)^2} \tag{7}$$

$$G_{Ep} = G(t) \tag{8}$$

$$G_{Mp} = \mu_P G(t) = 2.79 G(t). \tag{9}$$

The neutron form factors are

$$G_{En} = -\frac{\mu_N \tau}{1 + 5.6\tau} G(t) = \frac{1.91\tau}{1 + 5.6\tau} G(t) \tag{10}$$

$$G_{Mn} = \mu_N G(t) = -1.91 G(t). \tag{11}$$

These results reproduce reasonably well the form factors extracted by the Rosenbluth separation method. Data from studying the polarization transfer of polarized electrons to proton targets have yielded a different set of form factors [32]. For the total cross section and energy loss parameters, the new parametrizations yield essentially the same results as Eqs. (6)–(10) above.

The electric nuclear form factor [33], for large A, can be represented by [19,34]

$$G_E(t) = \frac{Z}{(1 + a^2 t/12)^2} \tag{12}$$

$$a = (0.58 + 0.82A^{1/3}) 5.07\ \mathrm{GeV}^{-1}. \tag{13}$$

For large A, we set $G_M \simeq 0$. This is a reasonable approximation because, roughly, the net magnetic moment of a multinucleon atom is small, and the prefactor of G_M in the cross section is also small.

The electric form factor associated with electron screening for hydrogen is obtained by using the electronic wave function to determine the charge density [33]. This leads to [19]

$$F_e(t) = \frac{1}{(1 + a_0^2 t/4)^2} \qquad (Z = 1). \tag{14}$$

Here, a_0 is the Bohr radius, $a_0 = 137/m_e$. For higher charge and atomic numbers (beyond helium), an approximate parametrization of the electronic electric form factor is [19,35]

$$F_e(t) = \frac{Z}{1 + a_e^2 t} \qquad (Z > 2) \tag{15}$$

$$a_e = 111.7 Z^{-1/3}/m_e. \tag{16}$$

For large Z, the dominant contribution to the elastic cross section is proportional to $(G_E - F_e)^2 \sim Z^2$ at short distances and large t; however, at large distances, $(G_E - F_e)^2 \sim 0$, where the nucleus is completely screened.

B. Incoherent scattering with nucleons and electrons

One component of the cross section for incoherent scattering to produce charged lepton pairs comes from elastic scattering with the individual protons and neutrons in the nucleus. Here, the target mass is $M_t = M$, and one parametrization of the structure functions gives

$$F_1^{\mathrm{incoh},N} = C(t)\frac{t}{2}(ZG_{Mp}^2 + (A - Z)G_{Mn}^2) \times \delta(M_X^2 - M^2) \tag{17}$$

$$F_2^{\mathrm{incoh},N} = C(t)\frac{t}{1 + t/4M^2}\Big(ZG_{Ep}^2 + (A - Z)G_{En}^2 + \frac{t}{4M^2}(ZG_{Mp}^2 + (A - Z)G_{Mn}^2)\Big)\delta(M_X^2 - M^2). \tag{18}$$

The prefactor $C(t)$ is the Pauli suppression factor. Following Tsai [19]

$$C(t) = \begin{cases} \frac{3Q_P}{4P_F}(1 - \frac{Q_P^2}{12P_F^2}) & Q_P < 2P_F \\ 1 & \text{otherwise,} \end{cases} \tag{19}$$

where $Q_P^2 = t^2/(4M^2) + t$ and $P_F = 0.25$ GeV.

There is scattering with the atomic electrons themselves [34]. For scattering with electrons, the target mass goes from M_A or M to m_e, and

$$F_1^{\mathrm{incoh},e} = \frac{t}{2} Z \delta(M_X^2 - m_e^2) \tag{20}$$

$$F_2^{\mathrm{incoh},e} = \frac{t}{1 + t/4m_e^2} Z\Big(F_e^{\mathrm{incoh}}(t) + \frac{t}{4m_e^2}\Big)\delta(M_X^2 - m_e^2). \tag{21}$$

For the hydrogen atom, $F_e^{\mathrm{incoh}} = 1 - F_e(t)^2$ with $F_e(t)$ given by Eq. (14). We use the parametrization of Ref. [34] for higher Z atoms, where

$$F_e^{\mathrm{incoh}} = \frac{c^4 t^2}{(1 + c^2 t)^2} \tag{22}$$

$$c = 724 Z^{-2/3}/m_e. \tag{23}$$

For the high energies of interest here, neglecting addition diagrams coming from identical particle exchange in $\mu e^- \to \mu e - e^+ e^-$ is an acceptable approximation [21].

C. Inelastic scattering with nucleons

For μA scattering where the momentum transfer is large enough that we are above threshold for pion production, inelastic scattering accounting for the substructure of the nucleons is required. For the proton structure function $F_2^p(x_{Bj}, t)$, we use the Abramowicz, Levin, Levy, and Maor [28] parametrization, updated in Ref. [29]. We do not include the parametrization here, but refer the reader to Ref. [29]. The parametrization also appears in an Appendix of Ref. [36]. This parametrization of the structure function is valid over the important range of small t, the dominant contribution to the inelastic cross section. It agrees well with data over a wide range of x_{Bj} and t including the perturbative regime.

For inelastic scattering with a nuclear target rather than a proton target, the process is still probing the structure of individual nucleons, so $M_t = M$. There is a nuclear effect that modifies the proton structure functions, called nuclear shadowing, which we incorporate with [37] $a(A, x_{Bj}, t) \simeq a(A, x_{Bj})$ and

$$a(A,x) = \begin{cases} A^{-0.1} & x_{Bj} < 0.0014 \\ A^{0.069\log_{10}x_{Bj}+0.097} & 0.0014 < x_{Bj} < 0.04 \\ 1 & 0.04 < x_{Bj}. \end{cases} \tag{24}$$

The nuclear structure functions are taken to be

$$F_2^A = a(A, x_{Bj})(Z + (A - Z)P(x_{Bj}))F_2^p \tag{25}$$

$$F_1^A = F_2^A/(2x_{Bj}), \tag{26}$$

where $P(x_{Bj}) = 1 - 1.85x_{Bj} + 2.45x_{Bj}^2 - 2.35x_{Bj}^3 + x_{Bj}^4$ accounts for the difference between proton and neutron structure functions [38].

III. RESULTS

A. Cross sections

We begin with muon scattering from protons to produce a pair of charged leptons. The cross section is the sum of the cross section for μp elastic scattering using the proton form factors in Eqs. (7)–(11) and the inelastic scattering term:

$$\sigma_{\mu p} = \sigma_p^{\rm coh} + \sigma_p^{\rm inel}. \tag{27}$$

For e^+e^- pair production shown in Fig. 2(a), the elastic scattering is ~5–6 orders of magnitude larger than the inelastic contribution. This can be understood by noting that the phase space integral with the photon propagator involves dt/t^2, making t near the minimum t the dominant part of the integral. The minimum t for elastic scattering is

$$t_{\rm min} \simeq \frac{4m_e^2m_\mu^2}{E^2},$$

as discussed in detail in, for example, Appendix A of Ref. [19]. The structure function $F_{2,p}^{\rm inel}$ is small for $t \ll M$.

The relevant scale for t is much larger for $m_e \to m_\tau$ in $\tau^+\tau^-$ pair production. Figure 2(b) shows that the inelastic contribution is comparable to the elastic cross section for a range of energies. The inelastic cross section contributes between 30% and 60% of the total cross section for muon energies between 10^2–10^9 GeV. Overall, however, the tau pair cross section is significantly smaller than the electron-positron pair production cross section. Tau pair production is not an important component of muon energy loss. Muon pair production is intermediate between the two sets of cross sections in Fig. 2 [25]. As noted above, we do not include muon pair production here due to the additional exchange diagram required by Fermi statistics for the identical fermions.

The targets of interest for atmospheric muons or muons produced by neutrinos are atoms. Figure 3(a) shows the contributions to the cross section from coherent scattering, incoherent scattering with electrons and nucleons, and inelastic scattering, for e^+e^- pair production by muons on a rock target, using the standard rock values of $A = 22$ and $Z = 11$. Figure 3(b) shows the same quantities for tau pair production.

For e^+e^- production, the coherent contribution dominates, followed by incoherent scattering on protons and electrons. Incoherent scattering with neutrons is at the level of $\sigma \sim 10^{-32}$–10^{-30} over the range of incident muon energies from 10–10^9 GeV. We note that our result for the incoherent scattering with atomic electrons agrees with the approximate analytic formula of Kel'ner in Eq. (46) of Ref. [21] to within 2% at $E_\mu = 100$ GeV, and is about 18% larger at $E_\mu = 10^9$ GeV for $Z = 11$. Our result for incoherent scattering with nucleons is a factor of ~10

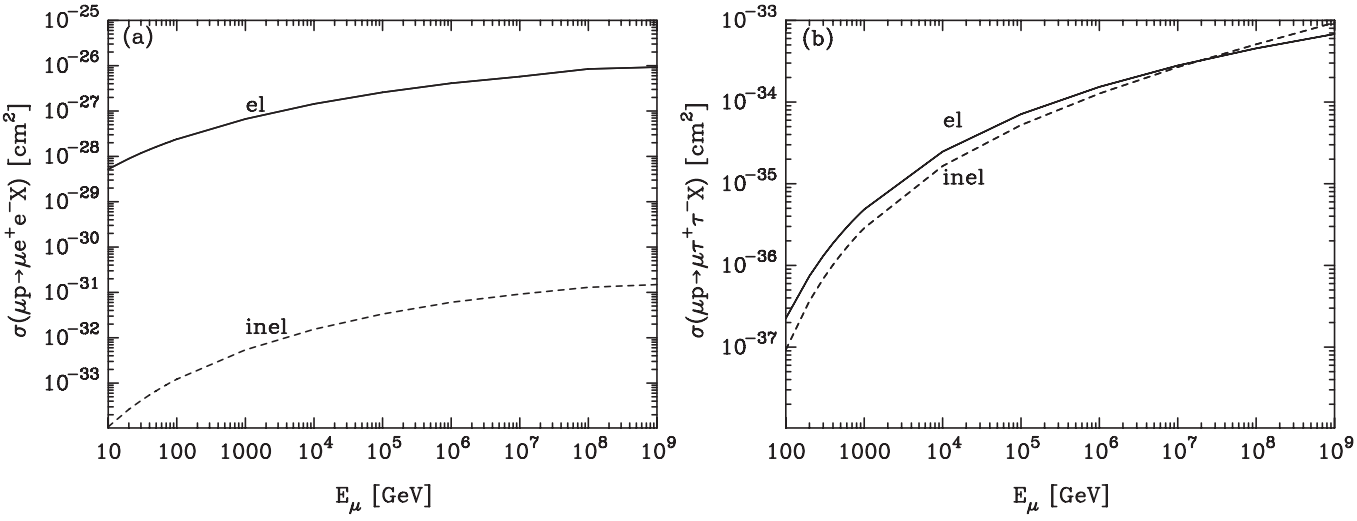

FIG. 2. Cross section for $\mu p \to \mu e^+ e^- X$ (a) and $\mu p \to \mu \tau^+ \tau^- X$ (b), showing the elastic and inelastic contributions separately.

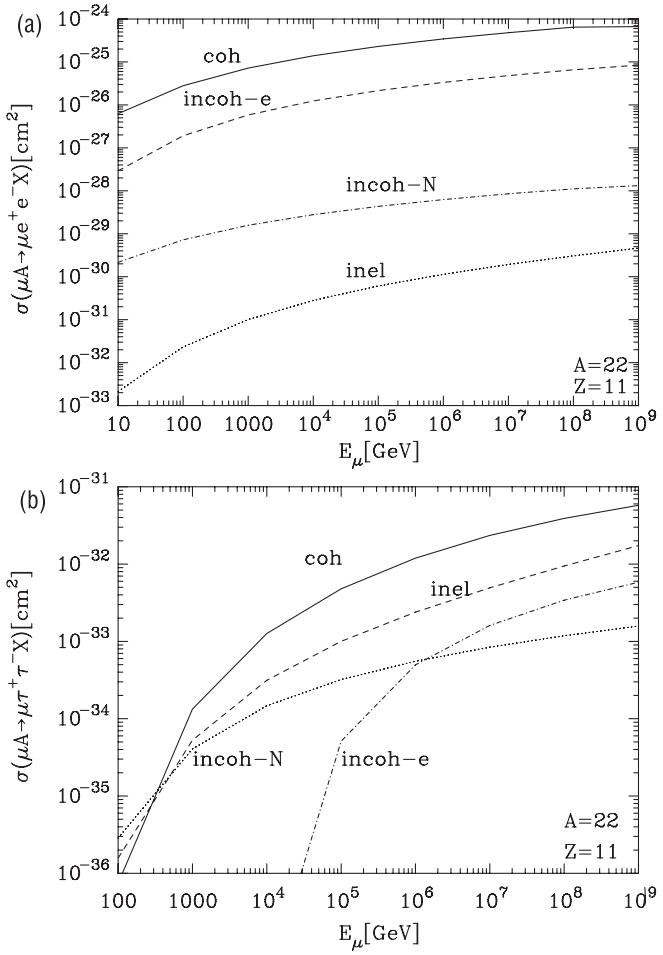

FIG. 3. Cross section for (a) $\mu A \to \mu e^+ e^- X$ and (b) $\mu A \to \mu \tau^+ \tau^- X$ for standard rock ($Z = 11$ and $A = 22$), for coherent, incoherent and inelastic contributions.

larger than in Ref. [34], in which the form factor is different. However, the consequences for e^+e^- pair production does not depend significantly on the incoherent nucleon contribution.

As in the case with proton targets, the inelastic contribution to e^+e^- pair production is orders of magnitude smaller than the elastic contribution. Tau pair production has a different balance of contributions. The coherent cross section dominates the total cross section to a lesser degree. As the muon energy increases well beyond the threshold for production of tau pairs in scattering with electrons, incoherent scattering with electrons becomes increasingly important. Inelastic scattering contributions are important, especially at the lower energies. Figure 3(b) shows the threshold energy dependence of the cross section for incoherent scattering with electrons. The Pauli suppression factor is particularly relevant in the evaluation of incoherent scattering with nucleons at high energies. Our result for incoherent scattering with nucleons is a factor of ~2–4 lower for tau pair production than the cross section coming from using the form factor in Ref. [34].

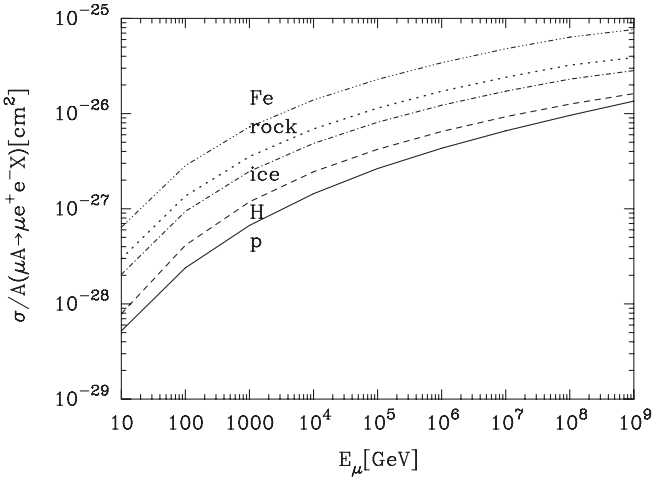

FIG. 4. Cross section divided by atomic number A for $\mu A \to \mu e^+ e^- X$, for $A = 1$ (proton and hydrogen), $A = 14.3$ (ice), $A = 22$ (standard rock), and $A = 55.9$ (iron).

The results for other targets are shown in Fig. 4, where the total e^+e^- pair production cross section is divided by A.

B. Energy loss parameter β_{pair}

The energy loss parameter β_{pair} is defined in Eq. (4). This parameter is shown in Fig. 5 for a variety of materials. For protons, β_{pair} rises with energy; however, for atomic targets with high energy muons, the atomic screening of the nucleus at large distances cuts off the growth of the parameter at high energies. The contribution to β_{pair} from tau pair production is suppressed by at least 4 orders of magnitude, depending on the muon energy.

Our evaluation of β_{pair} compares well with the analytical form of Kokoulin and Petrukhin (KP) [7,18]. At $E_\mu = 10$ GeV for rock, our result is 2.5% lower for β_{pair} than

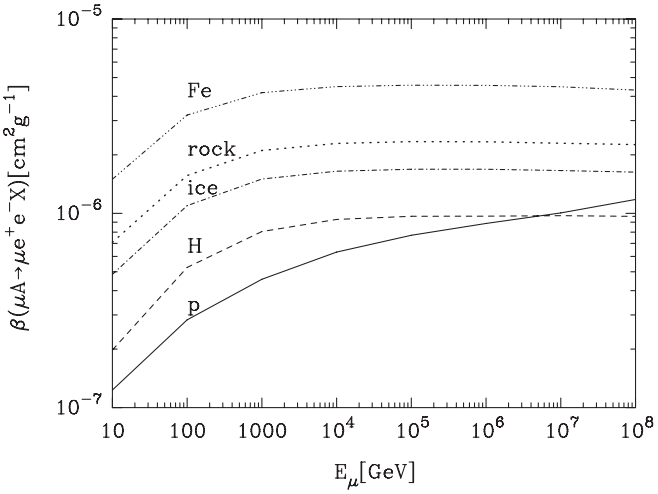

FIG. 5. Energy loss parameter β_{pair} via e^+e^- pair production for proton, hydrogen, ice, rock, and iron.

the KP evaluation. At 100 GeV, the two results agree to within <1%. At $E_\mu = 10^8$ GeV, our evaluation gives $\beta_{\rm pair}$ lower by ~4%. In the energy range of 10–100 GeV, our energy loss parameter is 2%–3% larger than that of Groom, Mokhov. and Striganov [9]. At $E = 10^5$ GeV, our results agree to within the numerical accuracy of our evaluation ($< 0.1\%$).

IV. DISCUSSION

One advantage of our approach is that we are not confined to the low t or small lepton mass limits. Although this is the dominant limit for the total cross section and the energy loss parameter for e^+e^- pair production, one can make interesting use of the formalism to consider high energy charged lepton pairs. The lepton pair energy (in the target rest frame) is

$$E_{\rm pair} = \frac{T + S_x}{2M_t} \tag{28}$$

in terms of invariants defined in the Appendix. Figures 6(a) and 6(b) show the total cross sections for lepton pair production by muons in ice, when the total pair energy is larger than 50 GeV.

As in the case of the total cross section, for e^+e^- pair production, the dominant contribution to the high energy pair cross section is coherent scattering with the nucleus, with a ~10% correction from incoherent scattering with the atomic electrons. The cross section for producing e^+e^- with $E_{\rm pair} = 50$ GeV for $E_\mu \sim 10^3$ GeV is $\sigma \sim 10^{-27}$ cm^2, equivalent to an interaction length of ~20 m. With the potential to measure electrons at this energy in IceCube, this may be an interesting reducible background to $\nu_e \to e$ conversions to electrons.

Tau pair production by 100 GeV muons has nearly equal contributions from coherent scattering, inelastic scattering, and incoherent scattering with nucleons. At high energies $E \sim 10^9$ GeV, the inelastic cross section is approximately half of the coherent cross section for 50 GeV tau pair production. Again, incoherent scattering with atomic electrons is about 10% of the cross section for coherent scattering when the muon energy is well above the threshold for tau pair production.

Tau neutrinos will come from the decays of tau pairs produced by muon transit through rock or ice. Tau neutrino production in the atmosphere is quite low, especially at low energies, because it requires heavy quark (charm or b quark) production [39,40]. Neutrino oscillations over the diameter of the Earth convert muon neutrinos to tau neutrinos. Tau decays from $\mu A \to \mu\tau^+\tau^- X$ will contribute to the overall downward flux of tau neutrinos. Quantitative evaluations of this source of downward-going tau neutrinos is under investigation.

In summary, we have provided a review of the contributions to e^+e^- and $\tau^+\tau^-$ production by muons as they interact electromagnetically as they pass through materials. Our approach is flexible, in that it can be applied to high momentum transfers, and to high mass leptons. Measurements of high energy e^+e^- pair production and tau pair (and associated tau neutrino pair) production will test the theoretical underpinnings of this evaluation.

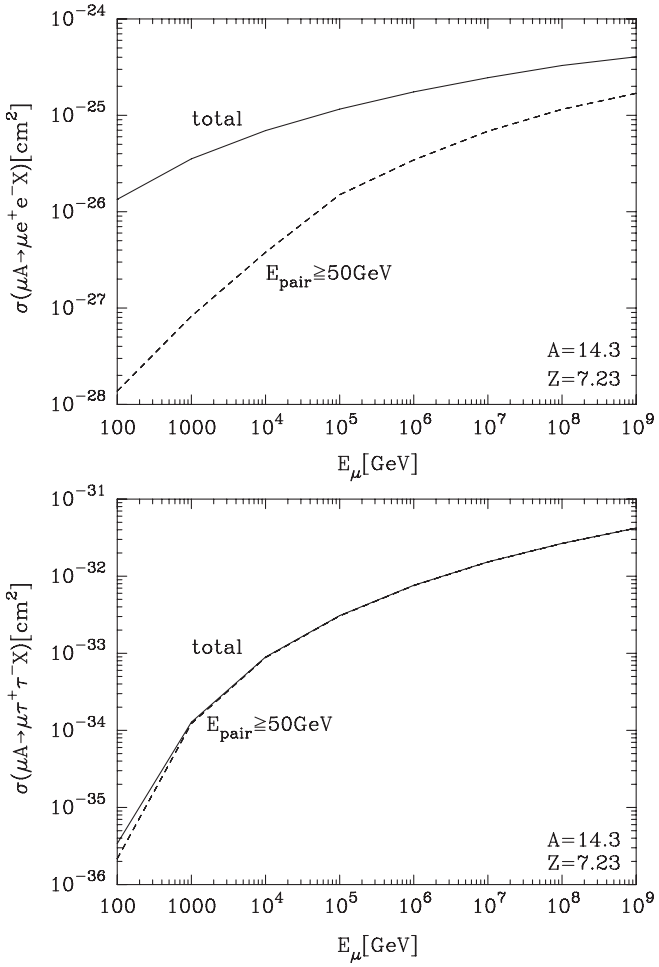

FIG. 6. Cross section for $\tau^+\tau^-$ pair production and for e^+e^- pair production for $E_{\rm pair} > 50$ GeV by muon interactions in ice.

ACKNOWLEDGMENTS

This research was supported in part by U.S. Department of Energy Contract No. DE-FG02-91ER40664. We thank F. Coester for helpful conversations.

APPENDIX A: KINEMATICS AND CROSS SECTION

We present here a compilation of useful kinematic relations and phase space limits for e^+e^- pair production on a proton target of mass M.

Figure 1 shows the dominant diagrams for $\mu(k) + P(p) \to \mu(k_1) + e(k_2) + \bar{e}(k_3) + X$, where

$$k + p = k_1 + k_2 + k_3 + \sum_x p_x.$$

Equation (3) shows the differential cross section in terms of phase space integrals and the quantities

$$Y = -Q^2 = -(k - k_1)^2 \qquad t = -q^2 = -(p - p_x)^2$$
$$\lambda_s = S^2 - 4m_\mu^2 M^2.$$

For the evaluation of the phase space, it is useful notationally to make the further definitions of invariants following Ref. [20]:

$$V^2 = \kappa^2 = (k_2 + k_3)^2 = (q + Q)^2 \qquad S = 2p \cdot k$$
$$X = 2p \cdot k_1 \qquad S_x = 2p \cdot Q = S - X \qquad M_x^2 = p_x^2$$
$$W^2 = (p + Q)^2 = M^2 + S - X - Y$$
$$T = 2p \cdot q = M^2 - t - M_x^2 \qquad \lambda_t = T^2 + 4M^2 t$$
$$\lambda_Y = S_x^2 + 4M^2 Y \qquad \Delta M^2 = (M_x^{\min} + 2m_e)^2 - M^2.$$

Rewriting the differential cross section [Eq. (3)]

$$d\sigma = \frac{1}{2\sqrt{\lambda_s}} A_{\alpha\beta} B_{\mu\nu}^{\alpha\beta} \frac{\alpha^4 W^{\mu\nu}}{2\pi^4 t^2 Y^2} d(PS), \tag{A1}$$

the phase space integrals reduce to

$$d(PS) = \frac{d\phi_1 dS_x dY dM_x^2 dt dV^2 d\phi_q}{16\sqrt{\lambda_Y \lambda_s}} d\Gamma_{\text{pair}}$$
$$d\Gamma_{\text{pair}} = \delta^4(\kappa - k_2 - k_3) \frac{d^3k_2}{2E_2} \frac{d^3k_3}{2E_3}$$
$$= \frac{1}{8}\sqrt{1 - 4m_e^2/V^2}\, d\cos\theta_e d\phi_e.$$

The limits of integration for these integrals are [20]

$$(M + m_\pi)^2 \le M_x^2 \le (\sqrt{W^2} - 2m_e)^2 \qquad 4m_e^2 \le V^2 \le \frac{1}{2M^2}(S_x T + \sqrt{\lambda_Y}\sqrt{\lambda_t}) - t - Y \qquad t_{\min} \le t \le t_{\max}$$
$$t_{\min} = (S_x(W^2 - M_x^2) + 2YM_x^2 - 4m_e^2(S_x + 2M^2) - \sqrt{U})/(2W^2)$$
$$t_{\max} = (S_x(W^2 - M_x^2) + 2YM_x^2 - 4m_e^2(S_x + 2M^2) + \sqrt{U})/(2W^2)$$
$$U = \lambda_Y(W^4 + M_x^4 + 16m_e^4 - 2(W^2(M_x^2 + 4m_e^2) + 4m_e^2 M_x^2)) \qquad Y^{\min} \le Y \le Y^{\max}$$
$$Y^{\min} = \frac{\lambda_s - SS_x}{2M^2} - \frac{1}{2M^2}\sqrt{(\lambda_s - SS_x)^2 - 4m_\mu^2 M^2 S_x^2} = \frac{\lambda_s - SS_x}{2M^2} - \frac{1}{2M^2}\sqrt{\lambda_s(\lambda_s - 2SS_x + S_x^2)} \qquad Y^{\max} = S_x - \Delta M^2$$
$$S_x^{\min} = [\lambda_s + \Delta M^2(S + 2M^2) - \sqrt{\lambda_s(\lambda_s - 2S\Delta M^2 + (\Delta M^2)^2 - 4m_\mu^2 \Delta M^2)}](2(S + m_\mu^2 + M^2))^{-1} \qquad S_x^{\max} = S - 2Mm_\mu.$$

Our numerical evaluation of these integrals was performed using the Fortran program VEGAS [41].

The integrals above are for inelastic scattering with a proton, hence the minimum $M_x^{2,\min} = (M + m_\pi)^2$.

Elastic scattering is enforced by a delta function of the form $\delta(M_x^2 - M_t^2)$, where M_t is the target mass. In this case, it is useful to rewrite the phase space integral involving $q = p - p'$ (for outgoing target momentum p') and $\kappa = k_2 + k_3$ as

$$d^4\kappa \delta^4(Q + q - \kappa) d^4q = \frac{1}{4\lambda_Y^{1/2}} dV^2 dt d(2p \cdot q) d\phi.$$

In the remaining integrals, for elastic scattering of a target of mass M_t, one makes the replacement $M \to M_t$. The target mass also appears in λ_s in Eq. (3).

We note that $q = p - p_x$ is the opposite sign to the usual convention. The Bjorken x value, $x_{Bj} = q^2/(2p \cdot q)$, in these variables is

$$x_{Bj} = \frac{t}{t + M_x^2 - M^2} = -\frac{t}{T}.$$

[1] T. DeYoung for the (IceCube Collaboration), J. Phys. Conf. Ser. **136**, 022046 (2008).
[2] A. Achterberg *et al.* (IceCube Collaboration), Phys. Rev. D **76**, 027101 (2007).
[3] M. Ambrosio *et al.* (MACRO Collaboration), Phys. Rev. D **52**, 3793 (1995).
[4] M. Ageron (ANTARES Collaboration), arXiv:0812.2095.
[5] See, for example, E. V. Bugaev, A. Misaki, V. A. Naumov, T. S. Sinegovskaya, S. I. Sinegovsky, and N. Takahashi, Phys. Rev. D **58**, 054001 (1998).
[6] S. I. Klimushin, E. V. Bugaev, and I. A. Sokalski, Phys. Rev. D **64**, 014016 (2001).
[7] W. Lohmann, R. Kopp, and R. Voss, CERN Yellow Report No. EP/85-03.
[8] P. Lipari and T. Stanev, Phys. Rev. D **44**, 3543 (1991).
[9] D. E. Groom, N. V. Mokhov, and S. Striganov, At. Data

Nucl. Data Tables **78**, 183 (2001).
[10] M. J. Tannenbaum, Nucl. Instrum. Methods Phys. Res., Sect. A **300**, 595 (1991).
[11] R. P. Kokoulin and A. A. Petrukhin, Nucl. Instrum. Methods Phys. Res., Sect. A **263**, 468 (1988); Sov. J. Part. Nucl. **21**, 332 (1990).
[12] V. B. Anikeev *et al.*, Proceedings of the 27th International Cosmic Ray Conference (ICRC 2001), Hamburg, Germany, 2001, p. 958.
[13] R. Gandhi and S. Panda, J. Cosmol. Astropart. Phys. 07 (2006) 011.
[14] G. Racah, Nuovo Cimento **14**, 93 (1937).
[15] N. F. Mott and H. S. W. Massey, *The Theory of Atomic Collisions* (Clarendon Press, Oxford, 1965).
[16] S. R. Kel'ner, Sov. J. Nucl. Phys. **5**, 778 (1967).
[17] S. R. Kel'ner and Yu. D. Kotov, Sov. J. Nucl. Phys. **7**, 237 (1968).
[18] R. P. Kokoulin and A. A. Petrukhin, in Proceedings of the XII International Conference on Cosmic Rays, Hobart, Tasmania, Australia, 1971, Vol 6.
[19] Y.-S. Tsai, Rev. Mod. Phys. **46**, 815 (1974).
[20] A. A. Akhundov, D. Yu. Bardin, and N. M. Shumeiko, Sov. J. Nucl. Phys. **32**, 234 (1980).
[21] S. R. Kel'ner, Yad. Fiz. **61**, 511 (1998) [Phys. At. Nucl. **61**, 448 (1998)].
[22] S. R. Kel'ner and D. A. Timashkov, Yad. Fiz. **64**, 1802 (2001) [Phys. At. Nucl. **64**, 1722 (2001)].
[23] G. R. Henry, Phys. Rev. **154**, 1534 (1967).
[24] M. J. Tannenbaum, Phys. Rev. **167**, 1308 (1968).
[25] V. Ganapathi and J. Smith, Phys. Rev. D **19**, 801 (1979).
[26] A. A. Akhundov, D. Yu. Bardin, N. D. Gagunashvili, and N. M. Shumeiko, Sov. J. Nucl. Phys. **31**, 127 (1980).
[27] S. R. Kel'ner, R. P. Kokoulin, and A. A. Petrukhin, Yad. Fiz. **63**, 1690 (2000) [Phys. At. Nucl. **63**, 1603 (2000)].
[28] H. Abramowicz, E. M. Levin, A. Levy, and U. Maor, Phys. Lett. B **269**, 465 (1991).
[29] H. Abramowicz and A. Levy, arXiv:hep-ph/9712415.
[30] R. Devenish and A. Cooper-Sarkar, *Deep Inelastic Scattering* (University Press, Oxford, 2004), p. 403.
[31] J. A. M. Vermaseren, arXiv:math-ph/0010025.
[32] For a review of recent results, see, e.g., C. F. Perdrisat, V. Punjabi, and M. Vanderhaeghen, Prog. Part. Nucl. Phys. **59**, 694 (2007).
[33] R. Hofstadter, Annu. Rev. Nucl. Sci. **7**, 231 (1957).
[34] Yu. M. Andreev and E. V. Bugaev, Phys. Rev. D **55**, 1233 (1997).
[35] L. Schiff, Phys. Rev. **83**, 252 (1951).
[36] S. I. Dutta, M. H. Reno, I. Sarcevic, and D. Seckel, Phys. Rev. D **63**, 094020 (2001).
[37] M. R. Adams *et al.* (E665 Collaboration), Phys. Rev. Lett. **68**, 3266 (1992); Phys. Lett. B **287**, 375 (1992); Z. Phys. C **67**, 403 (1995).
[38] A. C. Benvenuti *et al.* (BCDMS Collaboration), Phys. Lett. B **237**, 599 (1990).
[39] L. Pasquali and M. H. Reno, Phys. Rev. D **59**, 093003 (1999).
[40] A. D. Martin, M. G. Ryskin, and A. M. Stasto, Acta Phys. Pol. B **34**, 3273 (2003).
[41] G. P. Lepage, J. Comput. Phys. **27**, 192 (1978).
[42] D. Binosi and L. Theussl, Comput. Phys. Commun. **161**, 76 (2004).